Rheol Acta (2002) 41: 524–531
DOI 10.1007/s00397-002-0234-2

ORIGINAL CONTRIBUTION

Peter O. Brunn
Hesham Asoud

Analysis of shear rheometry of yield stress materials and apparent yield stress materials

Received: 21 August 2001
Accepted: 29 November 2001
Published online: 7 May 2002

P.O. Brunn (✉) · H. Asoud
Universität Erlangen-Nürnberg,
Lehrstuhl für Strömungsmechanik,
Cauerstraße 4, 91058 Erlangen, Germany
E-mail: pbrunn@lstm.uni-erlangen.de

Abstract For the most common types of viscometers the apparent flow curve of plastic fluids is studied. For torsional flow, where the shear rate is the natural variable, the apparent yield stress exceeds the true yield stress τ_c by more than 33%. If, on the other hand, τ is the natural variable (like in capillary flow, slit flow, and concentric cylinder flow) the yield stress is correctly predicted, but the behavior close to τ_c differs fundamentally. If the apparent shear rate $\dot{\gamma}_a$ goes to zero like $(\tau - \tau_c)^{1/n}$ (where the power law index n could be the power law index of a Herschel-Bulkley fluid), the true shear rate has to be proportional to $(\tau - \tau_c)^{[1/n]-1}$ for $\tau \to \tau_c$. For n = 1 this implies a discontinuity of $\dot{\gamma}$ at τ_c ($\dot{\gamma} = 0$ for $\tau < \tau_c$). For tangential annular flow between concentric cylinders the ratio of radii (κ) enters. Using an exact relation between $\dot{\gamma}$ and $\dot{\gamma}_a$ reveals that no single (κ-dependent) expression for the apparent flow curve can exist, which would for plastic fluids cover the entire flow regime ($\tau > \tau_c$). Irrespective as to what viscometer is used the far field behavior of the apparent flow curve and the true flow curve will, in general, differ too, though only quantitatively.

Keywords Plastic fluids · Flow curve · Apparent flow curve · Viscometry

Introduction

Plastic fluids constitute a class of frequently encountered fluids. Examples are concentrated suspensions, food stuffs, plaster, cement pastes, mortar, ceramic slices, pharmaceuticals, slurries, and so on. Frequently thixotropy accompanies the plastic behavior. Determining the viscosity of these fluids can be achieved either in the CR- or CS-mode. The latter has the advantage that the yield stress can be obtained without any extrapolation. Irrespective as to what mode is used it is necessary to manipulate the measured data (torque M and angular velocity in case of rotational viscometers) in order to obtain the flow curve. In the case of tangential annular flow between concentric cylinders the true flow curve can only be approximated (Krieger and Elrod 1953).

Without manipulation of the experimental data (like the Rabinowich-Mooney correction in capillary viscometry) one usually obtains only the apparent flow curve. Without exception this is the case if programs are used, which are supplied by the manufacturers of commercial instruments. One easy way to convert apparent flow curves into true ones relies on the *Method of Representative Shear Rate* and, respectively, representative shear *Stress* (MRSR/S). It was originally introduced by Schümmer (1969, 1970), who studied capillary flow of a power law fluid. He realized that if he shifted the apparent wall shear rate $\dot{\gamma}_a$ by a factor $\beta_c\left(=\frac{\pi}{4}\right)$ to the representative one, $\dot{\gamma} = \hat{\beta}_c \dot{\gamma}_a$, he could approximate the true flow curves within a 3% error for $0.25 \le n \le 1.4$. Since this error is within the scatter of experimental data the MRSR/S is extremely attractive to the practical everyday user. The method has been applied to other

viscometric devices and other model fluids as well (Giesekus and Langer 1977; Laun 1983; Laun and Hirsch 1989; Brunn and Vorwerk 1993; Caravalho et al. 1994). Its mathematical justification lies in the *Mean Value Theorem* (MVT) of integral calculus. Rigorously adhering to the MVT a model free estimate of β_c for the most common types of viscometers was recently presented (Brunn and Wunderlich 2000). For plastic fluids it turned out that a yield stress dependent shift factor is required. Thus, it is important to know if experimental data will furnish a yield stress an if so will this be the true yield stress.

To investigate this as well as the relation between apparent plastic flow curves and the true flow curve will be the subject of this study.

Plastic fluids in torsional flow

Plastic fluids are fluids with a yield stress τ_c, i.e., if the shear stress τ does not exceed τ_c, the plastic fluid will not flow (but only deform elastically) and the shear rate $\dot{\gamma}$ is zero. This implies that close to the yield stress the shear viscosity η, regarded as a function of $\dot{\gamma}$, has a singularity of order 1, i.e.,

$$\eta = \eta(\dot{\gamma}) \to \frac{\tau_c}{\dot{\gamma}} \text{ for } \tau \to \tau_{c+} \tag{1}$$

If we anticipate for $\tau > \tau_c$, at least close to the yield stress, a functional dependence of η upon $\dot{\gamma}$ of the form

$$\eta = \eta(\dot{\gamma}) = \frac{\left[\tau_c^s + m\dot{\gamma}^n\right]^{\frac{1}{s}}}{\dot{\gamma}},\ \mathrm{n} > 0 \tag{2}$$

then Eq. (1) is automatically satisfied. Equation (2) could also be regarded as a legitimate constitutive equation for plastic fluids, i.e., be valid not only close to τ_c.

It is a monotonically decreasing function of $\dot{\gamma}$ as long as $\frac{n}{s} \leq 1$ and implies a non-negative differential viscosity $\hat{\eta}$:

$$\hat{\eta} = \frac{d\tau}{d\dot{\gamma}} \geq 0 \tag{3}$$

Thus, subject to the restraint n/s ≤ 1, Eq. (2) can be used as a model for plastic fluids.

Some frequently used models for plastic fluids are special cases of Eq. (2). Examples are (for $\tau > \tau_c$):

1. The Bingham fluid

$$\tau = \tau_c + \eta_B\dot{\gamma} \tag{4a}$$

i.e., $m = \eta_B$, s = 1, n = 1

2. The Casson fluid

$$\sqrt{\tau} = \sqrt{\tau_c} + \sqrt{\eta_c\dot{\gamma}} \tag{4b}$$

i.e., $m = \sqrt{\eta_c}$, s = 1/2, n = 1/2

3. The Herschel Bulkley fluid

$$\tau = \tau_c + m\dot{\gamma}^n \tag{4c}$$

i.e., s = 1,

and

4. The Vocadlo fluid

$$\dot{\gamma} = \frac{1}{K}(\tau^s - \tau_c^s) \tag{4d}$$

i.e., m = K, n = 1

For torsional flow (flow between concentric parallel disks of radius R and distance H, rotating with angular velocity Ω relative to each other) the apparent viscosity η_a is given by

$$\eta_a = \eta_a(\dot{\gamma}_R) = \frac{\tau_a}{\dot{\gamma}_R} = C_1\frac{M}{\Omega} \tag{5}$$

with

$$C_1 = \frac{2H}{\pi R^4} \tag{6}$$

a purely geometrical quantity. Here M is the torque required to hold one disk stationary relative to the rotating one. With

$$\dot{\gamma}_R = \frac{R\Omega}{H} \tag{7}$$

the (ideal) rim shear rate, the apparent rim shear stress τ_a is given by (e.g., Bird et al. 1977)

$$\tau_a = \frac{4}{\dot{\gamma}_R^3}\int_0^{\dot{\gamma}_R} d\dot{\gamma}\dot{\gamma}^3\eta(\dot{\gamma}) \tag{8}$$

Utilizing Eq. (1) is follows that close to the yield stress, i.e., for $\dot{\gamma}_R \to 0$, τ_a is given by

$$\tau_a = \frac{4}{3}\tau_c,\ \text{for } \dot{\gamma}_R \to 0 \tag{9}$$

This implies that the apparent yield stress exceeds the true yield stress τ_c by more than 33%.

Utilizing Eq. (2) (with n/s ≤ 1) we obtain far from the yield stress

$$\tau_a \to \frac{4}{3+\frac{n}{s}}\tau_\infty,\ \text{for } \tau \gg \tau_c \tag{10}$$

where τ_∞ is the $\tau \gg \tau_c$ limit of Eq. (2), i.e.,

$$\tau_\infty = m^{\frac{1}{s}}\dot{\gamma}^{\frac{n}{s}} \tag{11}$$

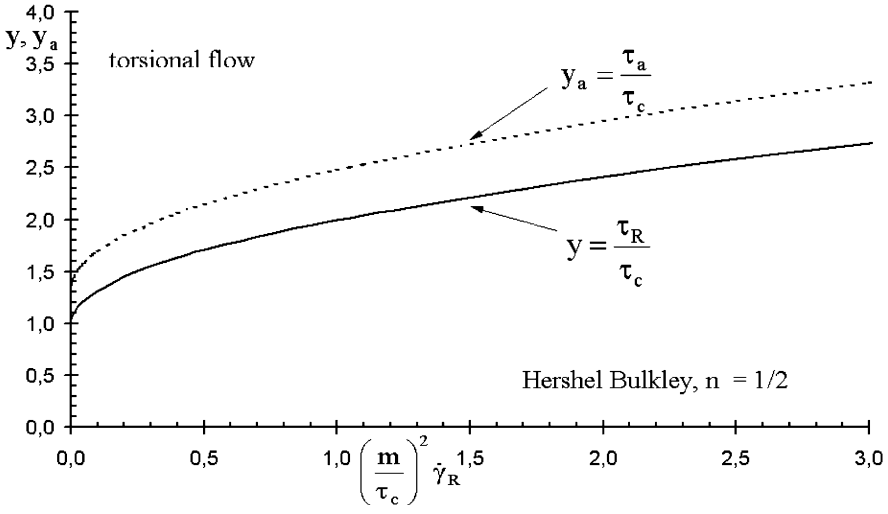

Fig. 1. The flow curve (*solid line*) and apparent flow curve (*dashed*) for torsional flow of a Herschel Bulkley fluid with n = 1/2

Thus, in torsional flow, the apparent viscosity η_a shows a first-order singularity in $\dot{\gamma}$ at an apparent yield stress of $\frac{4}{3}\tau_c$. Even the far field behavior ($\tau \gg \tau_c$) of η_a differs from the far field behavior of η, though only quantitatively by a factor of $\frac{4}{3+\frac{n}{s}}$.

For $\frac{n}{s} = 1$ (e.g., Bingham and Casson fluid), the far field behavior of η_a and η coincide. Figure 1 sketches the apparent flow curve ($\tau_a = \tau_a(\dot{\gamma})$) for a Herschel-Bulkley fluid[1] with n = 1/2.

Experimentally one measures M and Ω and thus η_a. Commercial instruments usually furnish parameters of approximation formulas for η_a, the apparent shear viscosity. Thus, it is instructive to find out the fluid's rheology, if η_a is approximated by formulas in the form of Eq. (2), i.e.,

$$\tau_a = \tau_a(\dot{\gamma}_R) = \left[\tau_c' s + m' \dot{\gamma}_R^n\right]^{\frac{1}{s}} \tag{12}$$

Here τ_c' is the apparent yield stress which, as shown before, exceeds the fluid specific yield stress τ_c by a factor of $\frac{4}{3}$. As the example of a Herschel Bulkley fluid has shown, the fluid specific property m can differ from an apparent quantity m′ as well (see footnote 1).

Inverting Eq. (8) leads to

$$\tau_R = \tau_R(\dot{\gamma}_R) = \frac{1}{4}\left[3 + \frac{d\log\tau_a}{d\log\dot{\gamma}_R}\right]\tau_a \tag{13}$$

If τ_a is approximated by Eq. (12), this implies

$$\tau_R = 1/4\left[3\tau_c' s + \left(3 + \frac{n}{s}\right)m'\dot{\gamma}_R^n\right]\left[\tau_c' s + m'\dot{\gamma}_R^n\right]^{(1-s)/s} \tag{14}$$

Thus, unless s = 1 (apparent Bingham and Herschel-Bulkley fluid), the fluids rheology functionally differs quite substantially from its apparent one[2]. Even for fluids with $\frac{n}{s} = 1$ (but s ≠ 1; e.g., Casson fluid), for which the far field behavior of τ_a and τ_R coincide (see Eq. 10), will the behavior of τ_a and τ_R for $\dot{\gamma}_R \to 0$ be quite different. Figure 2 shows this for an apparent Casson fluid:

$$\sqrt{\tau_a} = \sqrt{\tau_c'} + \sqrt{\eta_c'\dot{\gamma}_R}$$

for which one finds

$$\tau_R = 1/4\left(3\sqrt{\tau_c'} + 4\sqrt{\eta_c'\dot{\gamma}_R}\right)\left(\sqrt{\tau_c'} + \sqrt{\eta_c'\dot{\gamma}_R}\right) \tag{15}$$

Plastic fluids in capillary/slit flow

In capillary as well as in slit flow the experimentally accessible apparent viscosity is given by the analogue to Eq. (5), namely

$$\eta_a = \eta_a(\tau_w) = \frac{\tau_w}{\dot{\gamma}_a} = C_2\frac{\Delta p}{\dot{V}} \tag{16}$$

where C_2 is a purely geometrical constant. Here τ_w is the maximum (or wall) shear stress and $\dot{\gamma}_a$ the apparent shear rate given by (e.g., Brunn and Vorwerk 1993)

$$\dot{\gamma}_a = \frac{i+1}{\tau_w^i}\int_{\tau_c}^{\tau_w} d\tau\,\frac{\tau^i}{\eta(\tau)} \tag{17}$$

with i = 2 for slit flow and i = 3 for capillary flow.

This relation shows that for these flows the natural variable for η is the shear stress. Thus, Eq. (2) has to be used in the form

[1] For a Herschel Bulkley fluid τ_a is given by $\tau_a = \frac{4}{3}\tau_c + \left(\frac{4}{3+n}\right)m\dot{\gamma}_R^n$. This, too, is of the Herschel Bulkley type

[2] For s = 1 the apparent flow curve will differ from the true flow curve only quantitatively, but not qualitatively

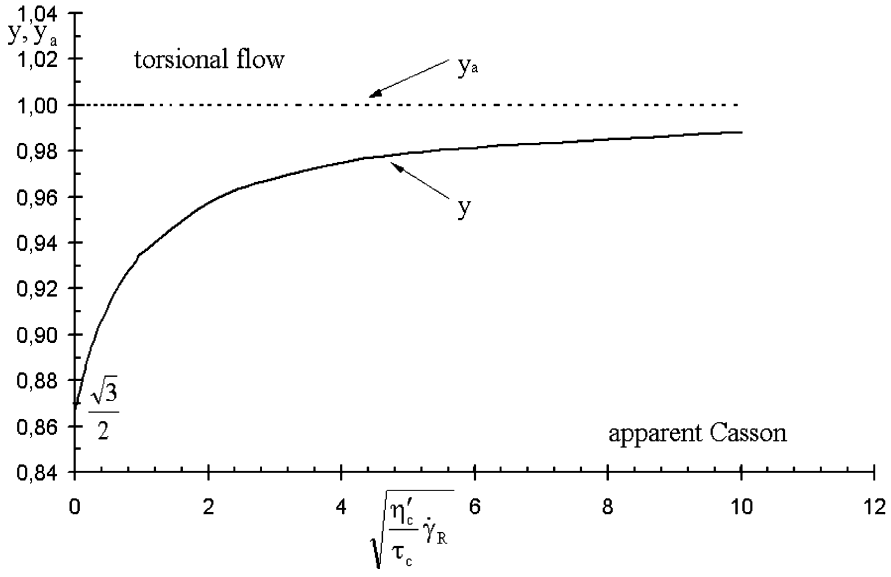

Fig. 2. Normalized Casson plot of a fluid, whose apparent flow curve (*dashed line*) in torsional flow shows Casson-like behavior; $y_a = \sqrt{\tau_a}/\left[\sqrt{\tau_c'} + \sqrt{\eta_c'\dot{\gamma}_R}\right] = 1$ in comparison to the scaled true flow curve (*solid line*) $y = \sqrt{\tau_R}/\left[\sqrt{\tau_c'} + \sqrt{\eta_c'\dot{\gamma}_R}\right]$

$$\eta = \eta(\tau) = \frac{\tau}{\left[\frac{1}{m}\left(\tau^s - \tau_c^s\right)\right]^{\frac{1}{n}}} \tag{18}$$

This implies for $\tau \to \tau_c$ the following expression for the shear viscosity:

$$\eta \to \frac{\tau_c}{\dot{\gamma}} = \left[\frac{m\tau_c^{n+1-s}}{s}\right]^{\frac{1}{n}} \frac{1}{(\tau - \tau_c)^{\frac{1}{n}}}, \text{ for } \tau \to \tau_c \tag{19}$$

i.e., a singularity of η of order 1/n for $\tau \to \tau_c$. Using Eqs. (17) and (19) the corresponding limiting behavior of η_a is

$$\eta_a \to \frac{\tau_c}{\dot{\gamma}_a} = \frac{n+1}{n(i+1)} \frac{\tau_c}{(\tau - \tau_c)} \eta, \text{ for } \tau \to \tau_c \tag{20}$$

This implies a singularity of η_a of order $1 + \frac{1}{n}$, i.e., of one order higher than the singularity of η.

Far from the yield stress, where $\dot{\gamma}$ becomes asymptotically equal to $\dot{\gamma}_\infty$,

$$\dot{\gamma}_\infty = \left(\frac{\tau^s}{m}\right)^{\frac{1}{n}}, \text{ for } \tau \gg \tau_c \tag{21}$$

we have

$$\dot{\gamma}_a = \left(\frac{i+1}{i+\frac{s}{n}}\right)\dot{\gamma}_\infty, \text{for } \tau_w \gg \tau_c \tag{22}$$

Thus, unless s/n = 1, as is the case for a Bingham and for a Casson fluid, the far field behavior of η_a will differ quantitatively from the far field behavior of η by a factor of (i + s/n)/(i + 1). For the physically meaningful range of $\frac{n}{s} \leq 1$ this implies $\eta_a/\eta \geq 1$. The apparent viscosity can never be less then the true viscosity, a result valid for torsional flow as well. Figure 3 illustrates this for a Vocadlo fluid with s = 2 in capillary flow.

Since, without exception, commercial instruments supply approximation formulas for apparent flow curves, it is instructive to show what this implies if the fluid is apparently a plastic one. To this end let us assume that the fluids apparent rheological behavior can be approximated by an analogue of Eq. (18), i.e.,

$$\dot{\gamma}_a = \left[\frac{1}{m'}\left(\tau_w^s - \tau_c^s\right)\right]^{\frac{1}{n}} \tag{23}$$

To obtain the true flow curve requires the inversion of Eq. (17). This is given by

$$\dot{\gamma}_w = \dot{\gamma}_w(\tau_w) = \frac{1}{i+1}\left[i + \frac{d\log\dot{\gamma}_a}{d\log\tau_w}\right]\dot{\gamma}_a \tag{24}$$

If the measured apparent shear rate turns out to be given by Eq. (23) then the true wall shear rate has to be

$$\dot{\gamma}_w = \frac{1}{i+1} \frac{\left[\left(i + \frac{s}{n}\right)\tau_w^s - i\tau_c^s\right]}{(m')^{1/n}} \left[\tau_w^s - \tau_c^s\right]^{(1/n)-1} \tag{25}$$

This shows that Eq. (23) can only be used for n ≤ 1.

For n = 1 (e.g., apparent Bingham and Vocadlo fluid), where $\dot{\gamma}_a(\tau_w)$ tends to zero linearly for $\tau_w \to \tau_{c+}$, Eq. (25) predicts a finite value for $\dot{\gamma}_w$. Phrased differently, only a finite value of η for $\tau \to \tau_{c+}$ (and $\eta = \infty$ for $\tau < \tau_c$) can lead to the behavior $\eta_a \propto \frac{1}{\tau - \tau_c}$ for $\tau \to \tau_{c+}$. If, on physical grounds, one rejects a discontinuity of $\dot{\gamma}$ (or η) at $\tau = \tau_c$, then all attempts to approximate η_a for plastic fluids via formulas, which admit a first order discontinuity (i.e., a proportionality of $\eta_a t_o(\tau - \tau_c)^{-1}$) for $\tau \to \tau_c$ should be abolished. Figure 4 illustrates this for an apparent Bingham fluid:

$$\dot{\gamma}_a = \begin{cases} 0, \tau_w < \tau_c \\ \frac{\tau_w - \tau_c}{\eta_B'}, \tau_w > \tau_c \end{cases}$$

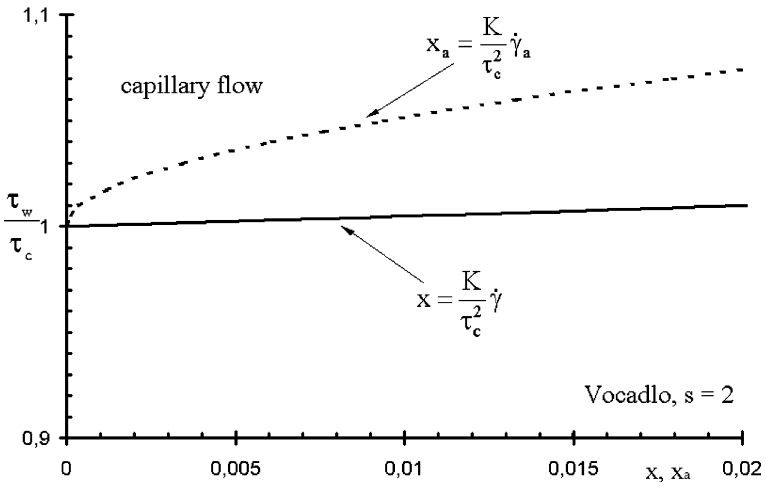

Fig. 3. The flow curve (*solid line*) and apparent flow curve (*dashed*) in capillary flow of a Vocadlo fluid with s = 2. Note the infinite slope of the apparent flow curve at the yield stress, while the slope of the true flow curve is 1/2 at τ_c

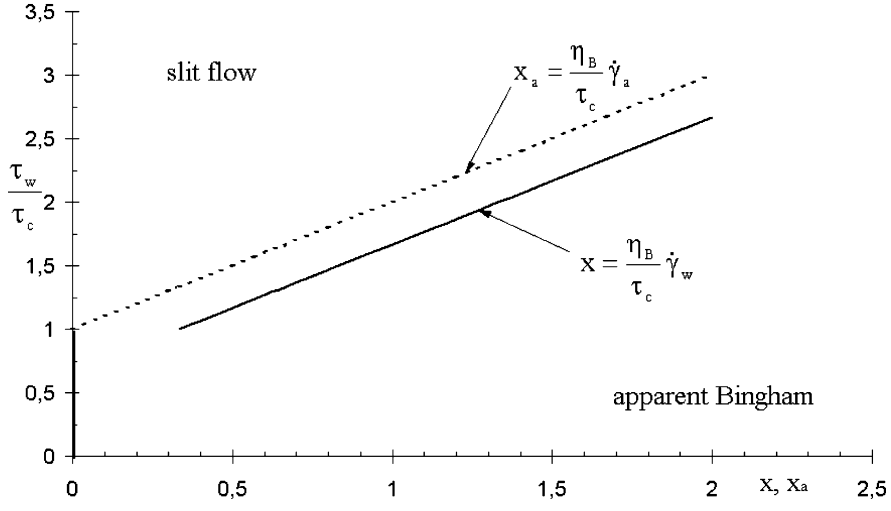

Fig. 4. Bingham plot of a fluid whose apparent flow curve (*dashed*) in slit flow shows Bingham behavior. Note the jump of the true wall shear rate $\dot{\gamma}_w$ (*solid line*) at the yield stress τ_c

for which the true rheology would be given by

$$\dot{\gamma}_w = \begin{cases} 0, \tau_w < \tau_c \\ \dfrac{\left(\tau_w - \frac{i}{i+1}\tau_c\right)}{\eta'_B}, \tau_w > \tau_c \end{cases} \tag{26}$$

Plastic fluids in angular flow between concentric cylinders

For this flow the apparent viscosity is given by

$$\eta_a = \eta_a(\tau_i;\kappa) = \frac{\tau_i}{\dot{\gamma}_a(\tau_i;\kappa)} = C_3\frac{M}{\Omega_r} \tag{27}$$

with Ω_r the angular velocity of one cylinder relative to the other (of radii R_i and $R_0 = \kappa R_i$, $\kappa > 1$) and M the torque per unit height required to maintain that situation. The constant C_3 is a purely geometrical quantity. Here τ_i is the shear stress at the inner cylinder. The apparent shear rate $\dot{\gamma}_a$ is directly related to Ω_r:

$$\dot{\gamma}_a = \frac{2\kappa^2}{\kappa^2 - 1}\Omega_r \tag{28}$$

With

$$\tau_0 = \tau_i/\kappa^2 \tag{29}$$

the shear stress at the outer cylinder, Ω_r is given by

$$\Omega_r = \begin{cases} \frac{1}{2}\int_{\tau_c}^{\tau_i} d\tau\dot{\gamma}/\tau, \tau_0 < \tau_c < \tau_i \\ \frac{1}{2}\int_{\tau_0}^{\tau_i} d\tau\dot{\gamma}/\tau, \tau_0 > \tau_c \end{cases} \tag{30}$$

These relations show that, in contrast to the cases studied thus far, apparent quantities ($\dot{\gamma}_a or \eta_a$) depend upon the geometry, though only via κ, the ratio of radii.

As seen above, τ is the natural variable and the results of the last section will (qualitatively) carry over. For example, close to the yield stress, where Eq. (19) holds, Eq. (20) has to be replaced by

$$\eta_a = \left(1+\frac{1}{n}\right)\left(1-\frac{1}{\kappa}\right)\frac{\tau_c}{\tau-\tau_c}\eta, \quad \text{for} \quad \tau_{\mathrm{i}} \to \tau_c \tag{31}$$

Far from the yield stress, the equivalent of Eq. (22) becomes

$$\dot{\gamma}_a = \frac{n}{s}\frac{\left(1-\kappa^{-2s/n}\right)}{\left(1-\kappa^{-2}\right)}\dot{\gamma}_\infty, \text{ for } \tau_0 \gg \tau_c \tag{32}$$

Fluid specific parameters enter this relation in the combination $\frac{n}{s}$. For $\frac{n}{s}=1$ (e.g., Bingham and Casson fluid) $\dot{\gamma}_a$ and $\dot{\gamma}_\infty$ coincide, irrespective of κ. In all other cases, $\dot{\gamma}_a$ differs quantitatively from $\dot{\gamma}_\infty$.

Again it is instructive to consider the case, where the apparent rheological behavior admits an approximation in the form of Eq. (23):

$$\dot{\gamma}_a = \left[\frac{1}{m'}\left(\tau_i^s-\tau_c^s\right)\right]^{\frac{1}{n}} \tag{33}$$

As is well known, Eq. (28) in conjunction with Eqs. (30a) and (30b) cannot be converted for arbitrary values of κ (the exception being $\kappa=\infty$). Thus, it seems impossible to extract information about the fluid rheology, which would lead to the validity of Eq. (33). However, if we concentrate on Eqs. (30a) and (30b) rather than on Eq. (28), then the inversion is straightforward and one gets for the true shear rate at the inner cylinder (Steger and Brunn 1999)

$$\dot{\gamma}_i = \begin{cases} 2\frac{d\Omega_r}{d\log\tau_i}, \tau_0 < \tau_c < \tau_i \\ 2\frac{\partial\Omega_r}{\partial\log\tau_i}\Big|_{\tau_0}, \tau_{\mathrm{c}} < \tau_0 \end{cases} \tag{34}$$

Thus, plotting the measured data half logarithmically as $\Omega_r = \Omega_r(\log\tau_i)$, the slope of that curve will furnish half of the true wall shear rate. For $\tau_c < \tau_0$ this requires fixed τ_0, i.e., a constant value of M/R_0^2. Writing Eq. (28) in the form

$$\Omega_r = \frac{1}{2}\frac{\tau_i-\tau_0}{\tau_i}\dot{\gamma}_a \tag{35}$$

shows the relation between $\dot{\gamma}_i$ and $\dot{\gamma}_a$, namely

$$\dot{\gamma}_i = \begin{cases} \left(1-\frac{1}{\kappa^2}\right)\frac{d\dot{\gamma}_a}{d\log\tau_i}, \tau_0 < \tau_c < \tau_i \\ \left[\frac{1}{\kappa^2}+\left(1-\frac{1}{\kappa^2}\right)\frac{\partial\log\dot{\gamma}_a}{\partial\log\kappa^2}\Big|_{\tau_0}\right]\dot{\gamma}_a, \tau_c < \tau_0 \end{cases} \tag{36}$$

In deriving these formulas we relied heavily on the fact that rheological quantities depend upon the fluid, but are independent of the geometry. Yet, as the expressions at Eq. (31) (for $\tau \to \tau_{c+}$) and Eq. (32) (for $\tau_0 \gg \tau_c$) show, the relation between $\dot{\gamma}_a$ and $\dot{\gamma}_i$ (and consequently between η_{a} and η) does involve κ. Insisting that $\dot{\gamma}_i$ does not depend upon κ requires a geometry dependent apparent shear rate $\dot{\gamma}_a = \dot{\gamma}_a(\tau_i, \tau_c; \kappa)$. As far as the approximation given by Eq. (33) is concerned, this can only be true if m′ is not a constant, but rather a function of κ.

As far as Eq. (36a) in concerned this requires

$$m' = m^*\left(1-\frac{1}{\kappa^2}\right)^{\mathrm{n}}, \quad \tau_{\mathrm{o}} < \tau_c < \tau_i \tag{37}$$

with m* a fluid specific constant.

The corresponding wall shear rate $\dot{\gamma}_i$ thus becomes

$$\dot{\gamma}_i = \frac{s}{n}\frac{\tau_i^s}{\tau_i^s-\tau_c^s}\left[\frac{1}{m^*}\left(\tau_i^s-\tau_c^s\right)\right]^{\frac{1}{n}}, \quad \tau_o < \tau_c < \tau_i \tag{38}$$

As in the case of capillary/slit flow the restraint $\mathrm{n}<1$ is needed for Eq. (33) to be applicable. For $\mathrm{n}<1$, Eq. (38) represents a plastic fluid, although not the same type as Eq. (18).

If we note that Eq. (33) with m′ given by Eq. (37) is equivalent to the approximation

$$\Omega_r = \frac{1}{2}\left[\frac{1}{m^*}\left(\tau_i^s-\tau_c^s\right)\right]^{\frac{1}{n}} \tag{39}$$

then it becomes clear, why this approximation cannot used for $\tau_o > \tau_c$. It is inconsistent with the correct expression for Ω_r (see Eq. 30b). Phrased differently, it is in the interval $\tau_o < \tau_c < \tau_i$ entirely legitimate to approximate experimental data by Eq. (33), if the κ-dependence of m′ as given by Eq. (37) is taken care of. Outside that range Eq. (33) cannot be used.

Within its range of validity ($n<1, \tau_{\mathrm{o}} < \tau_c < \tau_i$) the apparent shear rate varies between 0 (at $\tau_i = \tau_c$) and $\dot{\gamma}_{a,\max}$ (reached at $\tau_i = \kappa\tau_c$). The corresponding variation of the true wall shear rate $\dot{\gamma}_i$ is from 0 (unless $\mathrm{n}=1$) to $\frac{s}{n}\dot{\gamma}_{a,\max}$. Figure 5 shows details of these facts for an apparent Hershel-Bulkley fluid, i.e.,

$$\dot{\gamma}_a = \frac{1}{1-\frac{1}{\kappa^2}}\left[\frac{1}{m^*}\left(\tau_i-\tau_c\right)\right]^{\frac{1}{n}}, \quad \tau_o \le \tau_c \le \tau_i \tag{40}$$

It is instructive to note that for $\tau_i \to \tau_c$ the apparent flow curve $\tau_i = \tau_i(\dot{\gamma}_a)$ always has an infinite slope while the slope of the true flow curve varies between zero (for $\frac{1}{2} < n < 1$) and infinity for $n < \frac{1}{2}$. The value of $\frac{1}{2}$ for

$$n = \frac{1}{2}$$

separates these two cases.

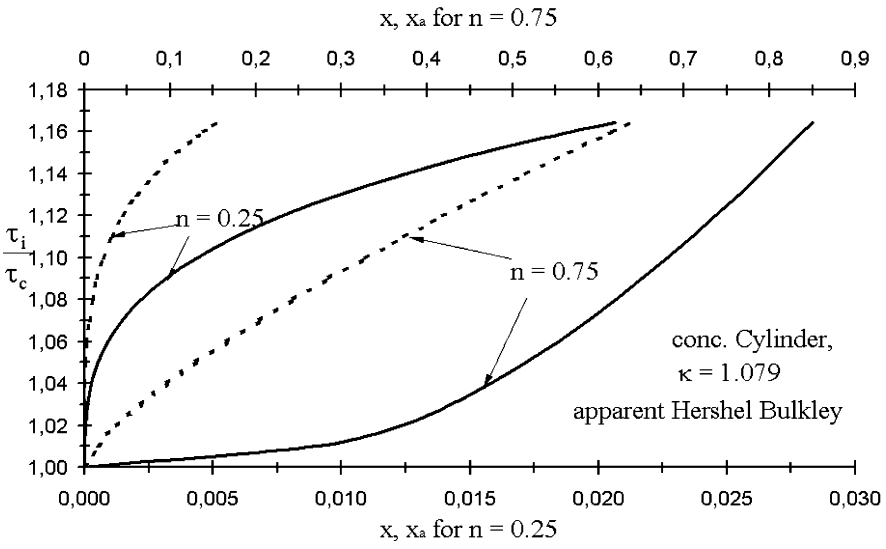

Fig. 5. The flow curve (*solid line*) and apparent flow curve (*dashed*) of a fluid in circular Couette flow ($\kappa = 1.079$, DIN 53018) with apparent Hershel-Bulkley behavior $\left(x_a = \dot{\gamma}_a \left(\frac{m^*}{\tau_c}\right)^{\frac{1}{n}}\right)$ in comparison to the true flow curve $\left(x = \dot{\gamma}_i \left(\frac{m^*}{\tau_c}\right)^{\frac{1}{n}}\right)$ for various values of n

Summary and conclusion

In this study the relation between flow curves and apparent flow curves was examined for plastic fluids. The results can be summarized as follows:

1. In viscometers, in which the shear rate is the natural variable (torsional flow), the yield stress is incorrectly predicted. The measurable apparent yield stress τ_{ac} exceeds the true yield stress τ_c by a factor of $\frac{4}{3}$. For $\dot{\gamma} \to 0$ the apparent viscosity η_a will tend to infinity as $\dot{\gamma}^{-1}$ at the apparent yield stress τ_{ac} while η will do likewise at the true yield stress τ_c. Even the far field behavior of η_a and η will differ, though only quantitatively by a factor of $\frac{4}{3+\frac{n}{s}}$. Since $n/s \leq 1$ this factor can never be less than one.
2. In capillary- and slit viscometers the yield stress is correctly predicted. The behavior close to the yield stress differs fundamentally, however. If, for $\tau \to \tau_c$, the shear rate vanishes like $(\tau - \tau_c)^{1/n}$, the apparent shear rate vanishes like $(\tau - \tau_c)^{[1/n]+1}$. Phrased differently, if the apparent shear rate turns out to vanish like $(\tau_w - \tau_c)^{1/n}$, then the true wall shear rate has to vanish like $(\tau_w - \tau_c)^{[1/n]-1}$. Thus, $n \leq 1$ is required in order to obtain meaningful results. For $n = 1$ (e.g., apparent Bingham fluid, apparent Vocadlo fluid) this implies a finite value of $\dot{\gamma}_w$ as $\tau \to \tau_{c+}$ (but $\dot{\gamma}_w = 0$ for $\tau_w \leq \tau_{c-}$). The corresponding jump of η (from infinity to a finite value) seems physically inadmissible, thus restricting for the apparent flow curve the range of n to values less than one. Again, the far field behavior of η_a and η will differ quantitatively, unless $\frac{n}{s} = 1$.
3. In tangential annular flow between concentric cylinders the results of 2. will carry over with one additional complication, namely the direct dependence upon the ratio of radii, κ. Using an exact differential relation between $\dot{\gamma}_a$ and $\dot{\gamma}$ reveals that a κ-dependent approximation formula for $\dot{\gamma}_a$ may – again only for $n < 1$ – be entirely legitimate, as long as the yield stress is encountered within the fluid filled space (i.e., for $\tau_o \leq \tau_c \leq \tau_i$). However is not legitimate to use that formula outside this range (i.e., for $\tau_c < \tau_0$). As a matter of fact, if we use the approximation of $\dot{\gamma}_a$ by Eq. (33) (with $m' = m'(\kappa)$ as given by Eq. (37) in its forbidden range $\tau_c < \tau_o$ we would obtain by Eq. (36b)

$$\dot{\gamma}_i = \left(\frac{\tau_i^s - \tau_c^s}{m'}\right)^{\frac{1}{n}} - \left(\frac{\tau_i^s - \kappa^{2s}\tau_c^s}{\kappa^{2s} m'}\right)^{\frac{1}{n}}, \tau_c < \tau_o \qquad (41)$$

There is no value for s and n, which would make this independent of κ. Programs from manufactures of commercial viscometers, which do furnish approximation formulas for apparent flow curves of plastic fluids for this type of flow, should be discarded.

In all cases the apparent viscosity η_a can never be less than the true viscosity η, i.e., $\eta_a/\eta \geq 1$.

References

Bird RB, Armstrong RC, Hassager O (1977) Dynamics of polymeric liquids, vol 1. Wiley, New York

Brunn PO, Vorwerk J (1993) Determination of steady-state shear viscosity from measurements of the apparent viscosity for some common types of viscometers. Rheol Acta 32:380–397

Brunn PO, Wunderlich T (2000) The role of the mathematical mean value theorem (MVT) in rheometry: an easy way to convert apparent flow curves into correct ones. Rheol Acta 39:384–391

Caravalho MS, Padmanabkan N, Macosko CW (1994) Single point correction for parallel disks rheometry. J Rheol 36:1925–1936

Giesekus H, Langer G (1977) Die Bestimmung der wahren Fließkurven nicht Newtonscher Flüssigkeiten und plastischer Stoffe mit der Methode der representativen Viskosität. Rheol Acta 16:1–22

Krieger IM, Elrod HJ (1953) Direct determination of the flow curves of non-Newtonian fluids. II. Shearing rate in the concentric cylinder viscometers. J Appl Phys 24:134–136

Laun HM (1983) Polymer melt rheology with a slit die. Rheol Acta 22:171–185

Laun HM, Hirsch G (1989) New laboratory tests to measure rheological properties of paper coatings in transient and steady-state flows. Rheol Acta 28:267–280

Schümmer P (1969) Zur Darstellung der Durchflußcharakteristik viscoelastischer Flüssigkeiten in Rohrleitungen. Chem Ing Tech 41:1020–1022

Schümmer P (1970) Zur Darstellung der Durchflußcharakteristik viscoelastischer Flüssigkeiten in Rohrleitungen. Chem Ing Tech 42:1239

Steger R, Brunn PO (1999) Wormlike micellar surfactant solutions: rheological and fluid mechanical oddities. In: Siginer DA, De Kee D, Chhabra RP (eds) Advances in the flow and rheology of non-Newtonian fluids, part A. Elsevier, Amsterdam, pp 119–136